

# 000 001 002 003 004 005 006 007 008 009 010 011 012 013 014 015 016 017 018 019 020 021 022 023 024 025 026 027 028 029 030 031 032 033 034 035 036 037 038 039 040 041 042 043 044 045 046 047 048 049 050 051 052 053 TC-MoE: AUGMENTING MIXTURE OF EXPERTS WITH TERNARY EXPERT CHOICE

**Anonymous authors**

Paper under double-blind review

## ABSTRACT

The Mixture of Experts (MoE) architecture has emerged as a promising solution for reducing computational overhead by selectively activating subsets of model parameters. The effectiveness of MoE models is primarily dependent on their routing mechanisms, with the widely adopted Top-K routing scheme used to activate experts. However, the Top-K scheme has notable limitations, including unnecessary activations and underutilization of existing experts. In this work, rather than modifying the routing mechanism as in previous studies, we propose Ternary Choice MoE (TC-MoE), a novel approach that expands the expert space by multiplying each expert with the ternary set  $\{-1, 0, 1\}$ . This expansion allows for more efficient and effective expert activations without incurring significant computational cost. Additionally, given the unique characteristics of the expanded expert space, we introduce a new load balancing loss and reward loss to ensure workload balance and achieve a flexible trade-off between effectiveness and efficiency. Extensive experiments demonstrate that TC-MoE achieves an average improvement of more than **1.1%** over the traditional approaches, while reducing the average number of activated experts by **up to 9%**. These results confirm that TC-MoE effectively address the inefficiencies of classical routing schemes, offering a more efficient and scalable solution for MoE-based large language models.

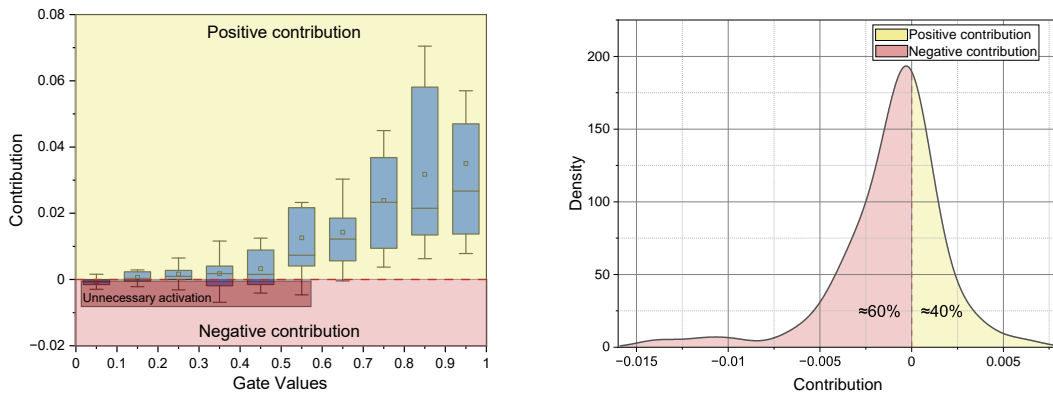
## 1 INTRODUCTION

In recent years, Large Language Models (LLMs) (Brown et al., 2020; Touvron et al., 2023; Achiam et al., 2023) have demonstrated impressive performance across a wide range of domains. However, modern LLMs still face inefficiencies, as they typically utilize all their parameters for every input token during both training and inference. This leads to a substantial increase in computing resource requirements as the models scale. To address these challenges, researchers have introduced the Mixture of Experts (MoE) architecture (Shazeer et al., 2017). The MoE architecture facilitates parameter scaling while maintaining reasonable computational expenses. Unlike traditional dense models, MoE models incorporate a routing mechanism that selectively activates specific subsets of parameters for particular input tokens. Recent advancements in MoE models (Jiang et al., 2024; Dai et al., 2024; Wu et al., 2024) have paved the way for scaling language models to unprecedented sizes and achieving remarkable performance enhancements.

Within the MoE architecture, the routing mechanism plays a critical role as it significantly influences both the efficiency and effectiveness of model training. Traditional MoE frameworks, such as GShard (Lepikhin et al., 2021), Switch Transformers (Fedus et al., 2022), and ST-MoE (Zoph et al., 2022) employ the Top-K routing scheme. This method calculates the routing probability for each expert with respect to every input token. The Top-K experts, selected based on the highest routing probabilities, are then activated for each input token. The output is the weighted sum of the outputs from the activated experts.

However, recent work (Zhou et al., 2022; Huang et al., 2024), along with our experiments, demonstrates that the Top-K routing scheme is suboptimal. We identify the following limitations:

- **Unnecessary Activations:** The Top-K scheme activates a fixed number of experts for each token, neglecting the possibility of adaptively choosing the number of activated experts. As



(a) Distribution of contributions from activated experts. The experts are categorized based on their gate values. This shows that some activations contribute negatively to the performance, indicating unnecessary activations.

(b) Distribution of contributions from experts with low gate values after flipping the sign of their outputs. The results demonstrate that some experts can positively impact performance when their output signs are flipped.

Figure 1: Analysis of the limitations in the conventional Top-K routing scheme in a model with 2 activated experts out of 8. We compute the contribution of each activated expert by measuring the difference in the model output quality when the activation is masked. More details of this figure are provided in Appendix A.1.

shown in Figure 1a, not all activated experts in the Top-K scheme contribute positively to the model’s performance, indicating the presence of unnecessary activations.

- **Underutilization of Existing Experts:** The Top-K scheme restricts experts to having only non-negative weights, disregarding the potential benefits of employing negative weights. As demonstrated in Figure 1b, approximately 40% of the experts with low gate values have positive contributions when their output signs are flipped.

In this work, we introduce **Ternary Choice Mixture of Experts (TC-MoE)** to address these limitations. Unlike previous studies (Zhou et al., 2022; Yang et al., 2024; Huang et al., 2024) that focus on modifying the routing scheme, we explore an alternative direction by expanding the expert space. Inspired by the concept of ternary quantization, where weights are projected to  $\{-1, 0, 1\}$ , we propose creating an expanded expert space by multiplying each expert in the original space with  $\{-1, 0, 1\}$ . As demonstrated in Figure 2b, by applying the ternary choice to each expert, we obtain an expanded expert space without increasing the parameter count of the experts. This expanded expert space enables the router to learn more complex routing strategies during the training process, thereby addressing the aforementioned limitations without modifying the routing scheme.

However, the expanded expert space exhibits unique characteristics that differ from the original expert space. As illustrated in Figure 2b, certain pairs of experts share the same parameters, while some experts have no parameter and incur no computational cost. Due to these differences, the traditional load balancing loss becomes unsuitable. To address this, we propose a new load balancing loss to ensure an equitable distribution of workload. Furthermore, based on our analysis, we introduce a novel reward loss to facilitate a flexible trade-off between efficiency and effectiveness.

We thoroughly evaluate our method using multiple common benchmarks. The results demonstrate that our TC-MoE outperforms all competitors. Compared to the baseline model, our method achieves an average improvement of **1.1%**, while reducing the average number of activated experts by **up to 9%**. When compared with other dynamic routing methods, our approach consistently achieves superior performance **under different activation budgets**. These results strongly confirm that TC-MoE effectively addresses the limitations of the classical routing scheme.

Our contributions can be summarized as follows:

1. We propose TC-MoE, a novel method to address the limitations of the classical routing scheme in MoE models. Unlike previous studies that focus on enhancing the routing

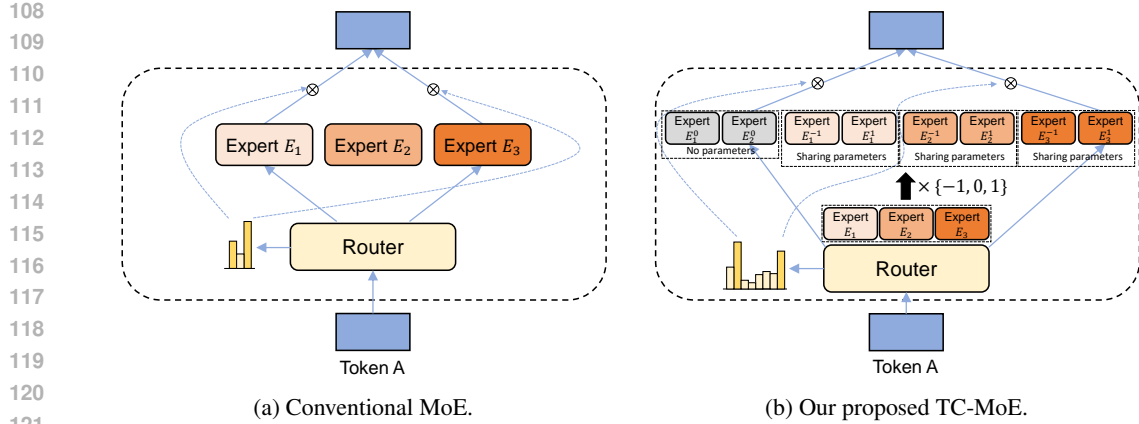


Figure 2: Comparison of conventional MoE and our TC-MoE. In this example, the original expert space comprises 3 experts, with a router activating 2 of them. By multiplying the original expert space with  $\{-1, 0, 1\}$ , TC-MoE obtains an expanded expert space with a total of 8 experts. Two experts have no parameter and incur no computational cost. The remaining experts are divided into three groups, with each group of experts sharing parameters.

scheme, TC-MoE leverages the concept of ternary quantization to expand the expert space without incurring significant costs. This expansion promotes more effective activations by the router.

- Given the unique load balance requirements in our expanded expert space, we redesign the load balancing loss. Additionally, we introduce a novel reward loss to achieve a flexible trade-off between effectiveness and efficiency.
  - Our experimental results demonstrate that TC-MoE achieves superior performance with fewer activated parameters, confirming significant improvements in both effectiveness and efficiency over the baseline.

## 2 RELATED WORK

**Mixture of Experts Models.** MoE models (Jacobs et al., 1991; Jordan & Jacobs, 1994) have been extensively studied in artificial intelligence. The concept of using a trainable gating network to determine a sparse combination of experts is pioneered by the Sparsely-Gated MoE (Shazeer et al., 2017). Since then, numerous studies (Lepikhin et al., 2021; Fedus et al., 2022; Zoph et al., 2022; Jiang et al., 2024; Dai et al., 2024; Wei et al., 2024) have built upon this framework, demonstrating compelling empirical results by scaling MoE models to unprecedented sizes.

**Routing Schemes.** The MoE architecture relies on a routing module to determine the activation of experts, making the routing scheme a critical factor for MoE model performance. Early works (Shazeer et al., 2017; Fedus et al., 2022) employ the Top-K routing scheme, which calculates the routing probabilities for each experts and activates the Top-K experts with the highest probabilities. Recent studies have focused on improving routing schemes. Zhou et al. (2022) introduce the expert choice routing mechanism, which assigns equal capacity to every expert and allows tokens to compete for expert selection. Yang et al. (2024) propose a threshold-based router that uses a manually set threshold to control the number of activated experts for each token. Huang et al. (2024) also propose a threshold-based router but take it a step further by incorporating a dynamic loss to prevent from activating too many experts.

**Heterogeneous Experts Design.** Unlike classical MoE frameworks that utilize feed-forward networks with the same configuration for all experts, recent works have explored the design of heterogeneous experts. Ainslie et al. (2023b) propose a heavy branch alongside a light branch, using a router to select important tokens for processing through the heavy branch. Raposo et al. (2024) further refine this concept in the decoder-only setting by defining the light branch as a skip connection.

162 Additionally, Zeng et al. (2024) introduce a set of null experts alongside ordinary experts, while  
 163 Wang et al. (2024) explore more diverse strategies for integrating heterogeneous experts.  
 164

165 In this paper, we propose TC-MoE, a novel method that complements existing research on routing  
 166 mechanisms in MoE models. Our framework provides a comprehensive design for expert spaces  
 167 by leveraging heterogeneous experts, thereby improving the overall performance and scalability of  
 168 MoE architectures.

### 169 3 METHOD

172 In this section, we begin with an overview of the widely-used Top-K routing mechanism in MoE  
 173 models. We then introduce our Ternary Choice MoE, a method that expands the expert space with  
 174 minimal computational overhead. Following this, we propose a new load balance loss function to  
 175 ensure effective load balance across the expanded expert space. Finally, we present a reward loss  
 176 technique that achieves a flexible trade-off between efficiency and performance in our approach.  
 177

#### 178 3.1 TOP-K ROUTING MECHANISM

179 In a typical MoE architecture for transformer language models, Feed-Forward Network (FFN) layers  
 180 are replaced with MoE layers. Each MoE layers consists of  $N$  independent FFNs, referred to as  
 181 experts,  $\{E_1, E_2, \dots, E_N\}$ , along with a trainable router. Given a hidden representation  $\mathbf{h} \in \mathbb{R}^d$  of  
 182 the input token, the router computes the probability distribution over the experts as follows:

$$183 \quad p(\mathbf{h}) = \text{Softmax}(\mathbf{W}_g \cdot \mathbf{h} + \mathbf{b}_g), \quad (1)$$

185 where  $\mathbf{W}_g \in \mathbb{R}^{N \times d}$  is a trainable weight matrix, and  $\mathbf{b}_g \in \mathbb{R}^N$  is the bias term. Then the Top-K  
 186 router selects the top  $K$  experts with the highest probabilities for each input token. The gate values  
 187 for the selected experts are set to the normalized probabilities, while those for the other experts are  
 188 set to 0:

$$189 \quad g_i(\mathbf{h}) = \begin{cases} p_i(\mathbf{h}) / \sum_{j \in \mathcal{E}} p_j(\mathbf{h}), & i \in \mathcal{E} \\ 0, & i \notin \mathcal{E} \end{cases} \quad (2)$$

192 where  $\mathcal{E}$  denotes the set of the top  $K$  experts with the highest probabilities. The final output  $O$  of  
 193 the MoE layer is computed as the weighted sum of the outputs from the activated experts:  
 194

$$195 \quad \mathbf{O} = \sum_{i \in \mathcal{E}} g_i(\mathbf{h}) \cdot E_i(\mathbf{h}). \quad (3)$$

#### 196 3.2 TERNARY CHOICE MOE

200 Although the Top-K routing scheme is widely used in MoE models, we argue that this method still  
 201 has notable limitations. As illustrated in Figure 1, the Top-K scheme suffers from unnecessary ac-  
 202 tivations, where some activated experts negatively impact model performance. It also underutilizes  
 203 existing experts, overlooking the potential benefits of contrasting expert outputs. While most previ-  
 204 ous studies focus on modifying the routing scheme to address these issues, we propose an alternative  
 205 approach, Ternary Choice MoE, which expands the expert space and provides the router a more di-  
 206 verse set of activation options. Specifically, as illustrated in Figure 2b, we augment the original  
 207 expert space by multiplying it with the ternary set  $\{-1, 0, 1\}$ . This allows us to project each expert  
 208  $E_i$  into three distinct experts  $\{E_i^{-1}, E_i^0, E_i^1\}$ , formulated as follows:

$$209 \quad E_i^1(\mathbf{h}) := E_i(\mathbf{h}), \quad E_i^0(\mathbf{h}) := 0, \quad E_i^{-1}(\mathbf{h}) := -E_i(\mathbf{h}), \quad \forall \mathbf{h} \in \mathbb{R}^d. \quad (4)$$

210 In this design, both  $E_i^1$  and  $E_i^{-1}$  share the same parameters as  $E_i$ . While  $E_i^0$  has no parameter  
 211 and is the same across all experts. We further simplify by maintaining only  $E_1^0, \dots, E_K^0$ , as this  
 212 is sufficient for the Top-K router to activate any number from 0 to  $K$  of these experts. **Therefore,**  
 213 **TC-MoE has totally  $2N + K$  experts.**

215 Our method only requires maintaining the parameters of  $E_i$ , consistent with the original model. The  
 only additional parameters and costs arise in the router. With the number of experts increased to

216  $2N + K$ , we introduce  $(N + K)d + N + K$  extra parameters and  $O((N + K)d)$  additional computational  
 217 costs in the router. However, this cost is negligible compared to the overall computational  
 218 cost of the MoE block.

219 For simplicity, we define the sets of each type of expert as follows:

$$220 \quad E^{-1} := \{E_i^{-1} | i \in [N]\}, \quad E^0 := \{E_i^0 | i \in [K]\}, \quad E^1 := \{E_i^1 | i \in [N]\} \quad (5)$$

222 Our method provides an alternative perspective for addressing the aforementioned limitations of  
 223 the Top-K routing scheme. Without altering the classical Top-K routing scheme, incorporating  $E^0$   
 224 allows the router to avoid unnecessary activations by activating experts from  $E^0$ , which contribute  
 225 zero to the output and incur no computational cost. Additionally, the inclusion of  $E^{-1}$  enables the  
 226 router to explore the potential benefits of flipping the signs of expert outputs.

227 Furthermore, we find that making a small improvement to the Top-K routing scheme by always  
 228 activating experts from  $E^0$  is beneficial. A detailed description of this improvement is provided in  
 229 Appendix A.3.

### 230 3.3 LOAD BALANCING LOSS

232 In common MoE models (Fedus et al., 2022; Zoph et al., 2022), an auxiliary loss is typically in-  
 233 troduced to encourage a balanced workload among experts. In our approach, however, experts are  
 234 categorized into two types:  $E^1 \cup E^{-1}$ , which incur computational costs, and  $E^0$ , which does not in-  
 235 cur any computational cost. Therefore, reasonable workload balance considerations in our scenario  
 236 are as follows: (1) experts from  $E^0$  do not need to be balanced with other experts since they do not  
 237 contribute to computational costs, and (2) the sum of the workloads of expert  $E_i^1$  and expert  $E_i^{-1}$   
 238 should be balanced, as  $E_i^1$  and  $E_i^{-1}$  are distributed on the same device in scenarios involving expert  
 239 parallelism (Lepikhin et al., 2021). Based on these considerations, we propose a new formulation  
 240 for the load balancing loss:

$$241 \quad f_i = \frac{1}{KT} \sum_{j=1}^T \mathbb{1}(\text{Token } j \text{ selects expert } E_i^1 \text{ or } E_i^{-1}), \quad (6)$$

$$245 \quad \bar{f} = \frac{1}{N} \sum_{i=1}^N f_i, \quad (7)$$

$$247 \quad p_i = \frac{1}{T} \sum_{j=1}^T \left[ p_{E_i^1}(\mathbf{h}_j) + p_{E_i^{-1}}(\mathbf{h}_j) \right], \quad (8)$$

$$250 \quad \mathcal{L}_{aux} = \sum_{i=1}^N (f_i - \bar{f}) \cdot p_i, \quad (9)$$

253 where  $T$  is the sequence length,  $f_i$  represents the sum of the activation frequencies of experts  $E_i^1$   
 254 and  $E_i^{-1}$ , and  $p_i$  denotes the sum of the average probabilities assigned to experts  $E_i^1$  and  $E_i^{-1}$ .

### 256 3.4 FLEXIBLE TRADE-OFF BETWEEN EFFICIENCY AND EFFECTIVENESS

258 Since  $E^0$  represents a special class of experts that incurs no computational cost, it is crucial to  
 259 understand how the router learns to allocate gate values to these experts. Based on our analysis,  
 260 we propose a novel auxiliary loss, termed the reward loss, to achieve a flexible trade-off between  
 261 efficiency and effectiveness by tuning the activated ratio of experts from  $E^0$ .

262 During the backward pass, the gradient of the gate value for each expert is computed as follows:

$$263 \quad \frac{\partial \mathcal{L}}{\partial g_i(\mathbf{h})} = \begin{cases} \left\langle \frac{\partial \mathcal{L}}{\partial \mathbf{O}}, E_i(\mathbf{h}) \right\rangle, & i \in \mathcal{E} \\ 0, & i \notin \mathcal{E} \end{cases} \quad (10)$$

267 For each activated expert  $E_i$ , the term  $-\frac{\partial \mathcal{L}}{\partial g_i(\mathbf{h})}$  indicates the impact of increasing the expert's gate  
 268 value on reducing the loss function. Since the sum of the gate values is constrained to 1, a compet-  
 269 itive dynamic arises among the activated experts. Experts that significantly contribute to reducing  
 the loss function are assigned higher gate values, as verified in Figure 1a.

Table 1: Comparison of performance across evaluation benchmarks. “Avg. K” denotes the average number of activated experts that incurs computational costs during inference. “#FLOPs  $\downarrow$ ” denotes the reduction ratio of FLOPs compared to the Top-K baseline. The **bold** number indicates the highest value for each benchmark.

| Pre-trained Dataset | Method                         | Avg. K | #FLOPs ↓ | ARC-Easy     | BoolQ        | MMLU         | LAMBADA      | HellaSwag    | OpenBookQA   | PIQA         | SQuAD        | WinoGrande   | Avg          |
|---------------------|--------------------------------|--------|----------|--------------|--------------|--------------|--------------|--------------|--------------|--------------|--------------|--------------|--------------|
| RedPajama           | <i>Base model</i>              |        |          |              |              |              |              |              |              |              |              |              |              |
|                     | Top-K                          | 2.00   | -        | <b>57.03</b> | 58.75        | 25.24        | <b>50.40</b> | 42.76        | 39.40        | 68.17        | 43.91        | 52.72        | 48.71        |
|                     | Random drop                    | 1.85   | 5.4%     | 56.48        | 58.62        | 25.35        | 50.13        | 42.83        | 39.00        | <b>69.53</b> | 44.68        | 51.30        | 48.66        |
|                     | Top-P                          | 1.99   | 0.3%     | 55.26        | <b>59.54</b> | <b>25.74</b> | 50.30        | 42.22        | 41.00        | 68.66        | 43.55        | 53.20        | 48.83        |
|                     | TC-MoE                         | 1.82   | 6.5%     | <b>57.03</b> | 59.20        | 25.58        | 50.16        | <b>43.51</b> | <b>42.00</b> | 68.66        | <b>44.88</b> | <b>54.85</b> | <b>49.54</b> |
|                     | <i>Fine-grained base model</i> |        |          |              |              |              |              |              |              |              |              |              |              |
|                     | Top-K                          | 4.00   | -        | 56.69        | 55.35        | 25.16        | 50.16        | 42.72        | 39.6         | <b>68.93</b> | 44.11        | <b>52.49</b> | 48.36        |
|                     | TC-MoE                         | 3.87   | 2.3%     | <b>57.58</b> | <b>58.56</b> | <b>26.80</b> | <b>50.46</b> | <b>43.16</b> | <b>41.80</b> | 68.28        | <b>45.19</b> | 52.09        | <b>49.32</b> |
|                     | <i>Tiny model</i>              |        |          |              |              |              |              |              |              |              |              |              |              |
|                     | Top-K                          | 2.00   | -        | 55.13        | 56.76        | 26.02        | 48.32        | 46.46        | 37.60        | 71.33        | 44.68        | 52.41        | 48.75        |
| FineWeb             | TC-MoE                         | 1.83   | 5.8%     | <b>55.93</b> | <b>58.53</b> | <b>26.2</b>  | <b>48.85</b> | <b>46.65</b> | <b>41.20</b> | <b>71.71</b> | <b>46.32</b> | <b>53.99</b> | <b>49.93</b> |
|                     | <i>Base model</i>              |        |          |              |              |              |              |              |              |              |              |              |              |
|                     | Top-K                          | 2.00   | -        | 60.19        | 50.76        | 26.46        | 53.95        | 53.23        | 43.00        | <b>74.48</b> | 45.60        | 55.33        | 51.44        |
|                     | TC-MoE                         | 1.86   | 5.1%     | <b>60.56</b> | <b>57.4</b>  | <b>26.67</b> | <b>54.01</b> | <b>54.05</b> | <b>44.00</b> | 73.43        | 47.24        | <b>56.12</b> | <b>52.61</b> |

Following Equation 10, for activated expert  $E_i^0$ , we have

$$\frac{\partial \mathcal{L}}{\partial g_{E_i^0}(\mathbf{h})} = \left\langle \frac{\partial \mathcal{L}}{\partial \mathbf{O}}, E_i^0(\mathbf{h}) \right\rangle = \left\langle \frac{\partial \mathcal{L}}{\partial \mathbf{O}}, \mathbf{0} \right\rangle = 0. \quad (11)$$

This indicates that expert  $E_i^0$  have no impact on reducing the loss function. Therefore, when competing with other activated experts, expert  $E_i^0$  will tend to receive higher gate values than experts with negative impacts but lower than those with positive impacts. This effectively helps in avoiding unnecessary activations.

Based on the above analysis, we propose extending our method to achieve a flexible trade-off between efficiency and effectiveness. Specifically, we manually assign a negative value to  $\frac{\partial \mathcal{L}}{\partial g_{E_i^0}(\mathbf{h})}$  instead of 0, thereby giving expert  $E_i^0$  a positive contribution in reducing the loss function. Consequently, the router will learn to promote the activation of these experts, while selectively deactivating other types of experts with minimal positive contributions. To achieve this, we introduce a new auxiliary loss, termed the reward loss, defined as follows:

$$\mathcal{L}_{rwd} = -\frac{1}{T} \sum_{i=1}^K \sum_{j=1}^T g_{E_i^0}(\mathbf{h}_j), \quad (12)$$

where  $T$  is the sequence length, and  $g_{E_i^0}(\mathbf{h}_j)$  represents the gate values of expert  $E_i^0$  on token  $\mathbf{h}_j$ .

Linearly combining the language modeling loss ( $\mathcal{L}_{lm}$ ), the load balance loss, and the reward loss, we yield the total loss, formulated as follows:

$$\mathcal{L} = \mathcal{L}_{lm} + \alpha_1 \mathcal{L}_{aux} + \alpha_2 \mathcal{L}_{rwd}, \quad (13)$$

where  $\alpha_1$  is a hyper-parameter known as the load balance factor, and  $\alpha_2$  is a hyper-parameter known as the reward factor.

## 4 EXPERIMENTS

## 4.1 EXPERIMENTAL SETTINGS

**Pre-trained Datasets.** We train our models using the RedPajama dataset (Computer, 2023) and the FineWeb dataset (Penedo et al., 2024). The RedPajama dataset includes diverse sources such as Common Crawl (CC), C4, Wikipedia, Github, books, arxiv, and Stackexchange. The FineWeb dataset is an open-source, high-quality training dataset consisting of cleaned and deduplicated English web data from CC. In our experiments, all models are trained on 100B tokens.

**Architecture.** We employ a decoder-only transformer model, primarily based on the LLaMA architecture (Touvron et al., 2023). Each transformer layer includes both an attention layer and an MoE layer. RMSNorm (Zhang & Sennrich, 2019) is applied to the inputs of both attention layers and MoE layers. Within the attention layer, we adopt the Group-Query Attention (GQA) (Ainslie et al., 2023a). Additionally, RMSNorm is used to normalize each key vector. Each FFN expert employs the SwiGLU activation function (Shazeer, 2020). In our experiments, We employ three types

324  
325  
326 Table 2: Configurations of our MoE models.  
327  
328  
329

| Model             | #Layers | #Hidden Size | #Heads | #KV Heads | #Intermediate Size | #Activated Experts/#Total Experts | #Activated Params/#Total Params |
|-------------------|---------|--------------|--------|-----------|--------------------|-----------------------------------|---------------------------------|
| Tiny              | 24      | 768          | 12     | 2         | 2048               | 2/8                               | 298M/978M                       |
| Base              | 32      | 1024         | 16     | 2         | 2816               | 2/8                               | 681M/2.3B                       |
| Fine-grained base | 32      | 1024         | 16     | 2         | 1280               | 4/16                              | 631M/2.1B                       |

330  
331 Table 3: Ablation study on the contribution of different types of experts. “Multiplication Set” de-  
332 notes the set used to multiply the original expert space, “Average K” denotes the average number of  
333 activated experts. Specifically, {1} represents the Top-K baseline.

| Multiplication Set | Average K | #FLOPs ↓ | Average Performance |
|--------------------|-----------|----------|---------------------|
| {1}                | 2.00      | -        | 48.71               |
| {-1, 1}            | 2.00      | 0.0%     | 49.00 (+0.29)       |
| {0, 1}             | 1.81      | 6.9%     | 49.23 (+0.52)       |
| {-1, 0, 1}         | 1.82      | 6.4%     | 49.54 (+0.83)       |

341  
342  
343 of models: tiny, base, and fine-grained base. Table 2 summarizes their respective configurations.  
344 We use the same tokenizer as GPT-NeoX-20B (Black et al., 2022), which has a vocabulary size of  
345 50257.346 Competitors. We pre-train three baseline methods alongside our proposed TC-MoE using the afore-  
347 mentioned architecture:

- 348
1. **Top-K**: A standard Top-K routing scheme that activates the top  $K$  experts for each token.  
349 We select  $K = 2$  or  $K = 4$  as these are the most common configurations in modern MoE  
350 architectures (Zoph et al., 2022; Jiang et al., 2024; Wei et al., 2024; Wu et al., 2024).
  2. **Random drop**: A variant of the Top-K routing scheme that, with probability  $p$ , does not  
353 activate the expert with the second highest probability.
  3. **Top-P**: The Top-P routing scheme (Huang et al., 2024), which activates the smallest set of  
355 experts whose cumulative probabilities surpass a threshold  $P$  for each token.
  4. **TC-MoE**: Our proposed method, which expands the expert space and adopts the standard  
358 Top-K routing scheme to activate the top  $K$  experts within this expanded expert space for  
359 each token.

360 The Top-K baseline adopts a fixed number of activated experts, whereas Random drop, Top-P, and  
361 TC-MoE allow for a flexible trade-off between effectiveness and efficiency by tuning specific hyper-  
362 parameters. Details of these hyper-parameters are provided in Appendix A.2.363  
364 **Evaluation.** We evaluate these models on seven different benchmarks: ARC (Clark et al., 2018),  
365 BoolQ (Clark et al., 2019), MMLU (Hendrycks et al., 2021), LAMBADA (Paperno et al., 2016),  
366 HellaSwag (Zellers et al., 2019), OpenBookQA (Mihaylov et al., 2018), PIQA (Bisk et al., 2020),  
367 SIQA (Sap et al., 2019), and Winogrande (Sakaguchi et al., 2021). These tasks examine mod-  
368 els’ logical reasoning, language understanding, commonsense reasoning, and knowledge utilization.  
369 Additionally, we measure the average number of activated experts that incur computational costs to  
370 demonstrate the efficiency of each model. Note that in our TC-MoE, only the activations of  $E^{-1}$   
371 and  $E^1$  are counted since  $E^0$  incurs no computational cost. For simplicity, we refer to the average  
372 number of activated experts as the average number of activated experts that incur computational  
373 costs in the following sections.374  
375 4.2 MAIN RESULTS376 Table 1 summarizes the performance of various models across different evaluation benchmarks.  
377 The results highlight the superior performance of our proposed TC-MoE compared to competing  
378 methods.

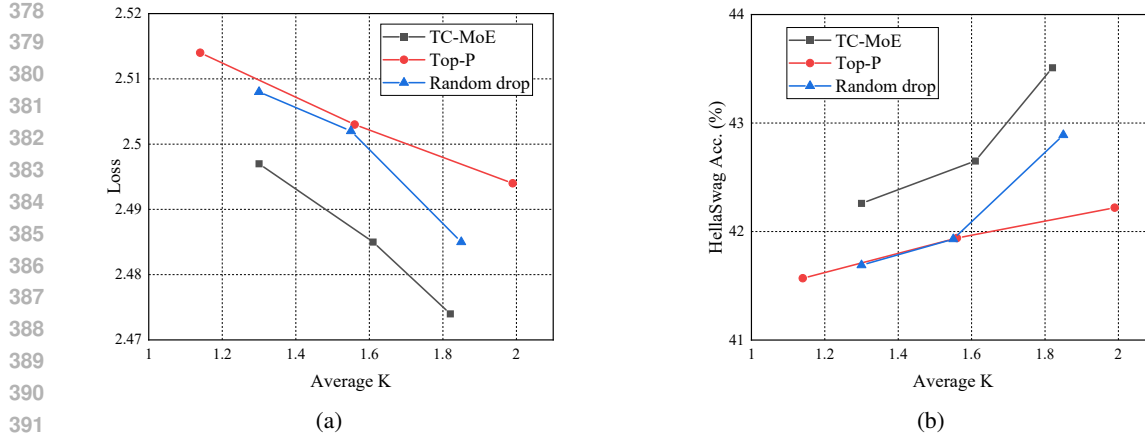


Figure 3: Comparison of (a) the language modeling loss and (b) the HellaSwag accuracy under different budgets for the average number of activated experts. The results demonstrate TC-MoE outperforms other competitors under all settings.

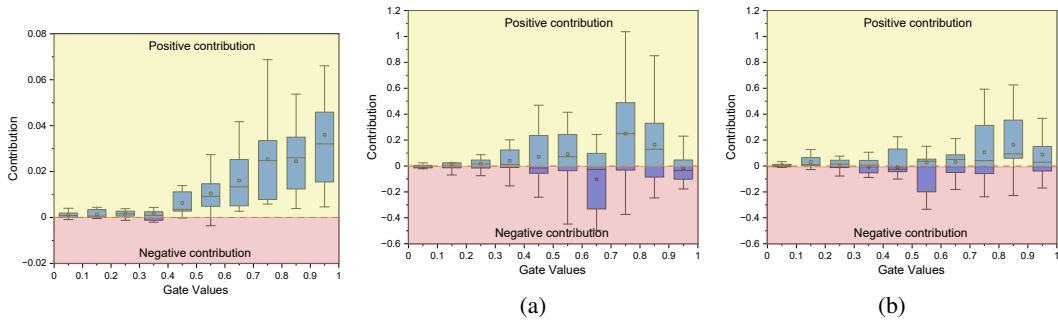


Figure 4: Distribution of contributions from activated experts in TC-MoE on pre-trained data.

Figure 5: Distribution of contributions from activated experts in (a) baseline and (b) TC-MoE on ARC-Easy. The results show a significant alleviation of unnecessary activations by TC-MoE.

Specifically, when pre-trained the base model on the RedPajama dataset, TC-MoE outperforms competitors on ARC-Easy, HellaSwag, OpenBookQA, SIQA, and WinoGrande, while achieving comparable results on BoolQ, MMLU, LAMBADA and PIQA. Notably, TC-MoE achieves an average accuracy of 49.54%, surpassing the Top-K baseline by 0.83%, Random drop by 0.88% and Top-P by 0.71%. For the fine-grained base model pre-trained on the RedPajama dataset, TC-MoE also outperforms the Top-K baseline, improving the average accuracy by 0.96%.

When pre-training on the FineWeb dataset, TC-MoE demonstrates even greater accuracy improvements. For the tiny model, TC-MoE surpasses the Top-K baseline by 1.18%. Similarly, for the base model, TC-MoE outperforms the Top-K baseline by 1.17%.

Beyond improved accuracy, TC-MoE consistently demonstrates greater efficiency. Specifically, it reduces the average number of activated experts by 9.0% and the required FLOPs by 6.5% compared to the Top-K baseline on the base model pre-trained on the RedPajama dataset. On the FineWeb dataset, TC-MoE reduces the average number of activated experts by 7.0% and the required FLOPs by 5.1%. These results demonstrate that our method achieves significant gains in both effectiveness and efficiency over the Top-K baseline.

Additionally, we conduct a thorough comparison of these methods under different budgets for the average number of activated experts. The results are shown in Figure 3. The figure demonstrates that the TC-MoE consistently outperforms the other two competitors across all settings regarding the average number of activated experts. Notably, in terms of the language modeling loss, TC-MoE reduces the loss by approximately 0.017 compared to competitors. For HellaSwag accuracy, TC-MoE improves accuracy by up to 0.7% compared to other methods.

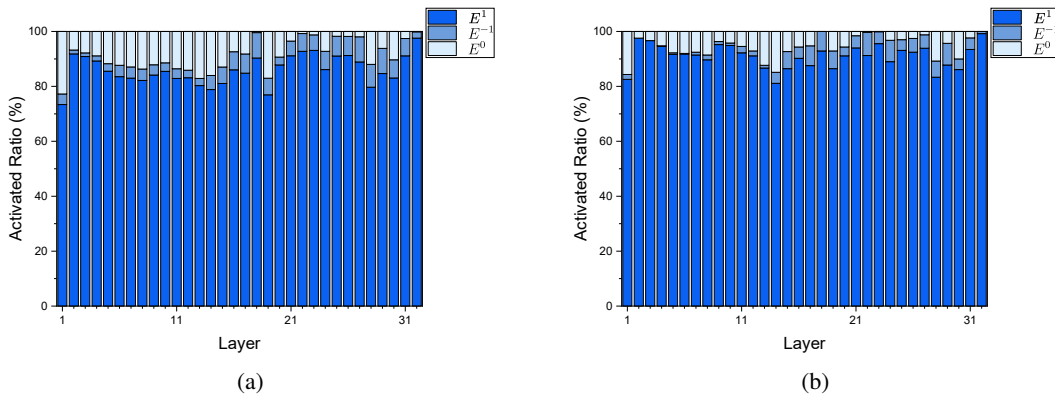


Figure 6: The activated ratio of different types of experts across layers on (a) the pre-trained data and (b) the test data (ARC-Easy). The results show a similar activated pattern on different data.

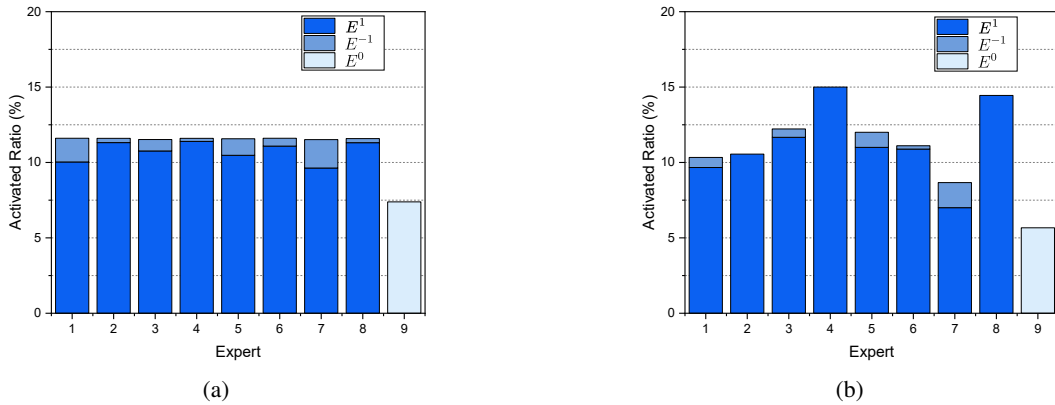


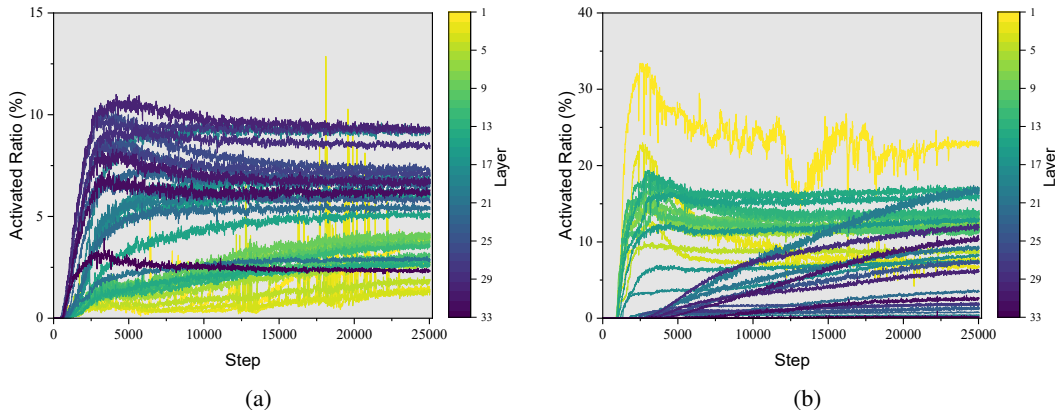
Figure 7: The activated ratio of different experts in layer 16 on (a) the pre-trained data and (b) the test data (ARC-Easy). The results show the effectiveness of our load balance loss during both training and inference.

### 4.3 ABLATION STUDY

We conduct an ablation study by evaluating the performance of our method using only a subset of  $\{-1, 0, 1\}$  to multiply the original expert space. As demonstrated in Table 3, expanding the expert space with either  $\{-1, 1\}$  or  $\{0, 1\}$  improves the model performance. Specifically, expanding the expert space with  $\{-1, 1\}$  results in an average performance increase of  $0.29\%$  while the average number of activated experts remains at 2.0. When expanding the expert space with  $\{0, 1\}$ , the average performance increase by  $0.52\%$ , and the average activated experts reduced by 0.19. When expanding the expert space with the complete set  $\{-1, 0, 1\}$ , the model achieves the best performance, with both improved results and a reduced number of activated experts. In summary, both type  $E^{-1}$  and type  $E^0$  contribute to the improvement of model performance, while type  $E^0$  also significantly enhances model efficiency.

### 4.4 ANALYSIS

**Unnecessary Activations.** We investigate the effect of our method on addressing unnecessary activations. Figure 4 shows the distribution of contributions from activated experts in TC-MoE on the pre-trained data. Compared to the distribution of contributions in the baseline model, shown in Figure 1a, our TC-MoE significantly alleviates the occurrence of unnecessary activations. Additionally, when analyzing unnecessary activations on ARC-Easy, we observe many more activations that contribute negatively. In this scenario, as shown in Figure 5, TC-MoE alleviates the occurrence of unnecessary activations even more significantly.

Figure 8: The changing curves of activated ratios of (a) type  $E^{-1}$  and (b) type  $E^0$  of different layers.

**Activated Ratio of Different Types of Experts.** To analyze the activated ratio of different types of experts, we visualize the activated ratios across layers in TC-MoE. The results are shown in Figure 6. We observe that type  $E^1$  has the highest activated ratio, indicating a major contribution to the output. Additionally, the model spontaneously learns to allocate around 20% activated ratio to type  $E^0$  and type  $E^{-1}$ , highlighting the necessity of these experts for more powerful routing. [The activation ratios on ARC-Easy are similar as that on pre-trained data, demonstrating the generalization of our method.](#)

The distribution of activated ratios varies significantly across different layers. Figure 8 visualizes the changing curves of the activated ratios across layers during the entire training process. We find that the activation ratios of type  $E^{-1}$  and type  $E^0$  across layers exhibit a converse pattern. For type  $E^{-1}$ , the model tends to activate more of them in the deeper layers. In contrast, type  $E^0$  is primarily activated in the shallow layers.

**Load Balance.** To explore the effectiveness of our load balancing loss, we visualize the activated ratios of different experts in our model during the training process. Figure 7 shows the activated ratios in layer 16. To observe the actual load balancing distribution, we stack the activated ratios of each  $E_i^{-1}$  and  $E_i^1$ , as they are distributed on the same device when involving expert parallelism. Additionally, we plot the sum of the activated ratio of type  $E^0$  at the position of expert 9, since they do not contribute to computational costs. We observe that our TC-MoE achieves a near-perfect workload balance with our designed load balancing loss [on the pre-trained dataset](#). The sum of the workloads of experts  $E_i^1$  and experts  $E_i^{-1}$  are balanced, each around 11.5%. Additionally, the activated ratios of expert  $E_i^1$  and expert  $E_i^{-1}$  are not fixed but are [instead learned dynamically](#) by the model. Furthermore, experts from  $E^0$  do not participate in the load balancing, allowing the model to activate  $E^0$  without any constraints. [On ARC-Easy, we observe a slight deviation in load balance, with the maximum expert workload reaching approximately 15.0%, while the minimum workload is around 8.5%](#).

## 5 CONCLUSIONS

In this paper, we present Ternary Choice MoE (TC-MoE), a novel approach designed to address the limitations of traditional Top-K routing in MoE architectures. By expanding the expert space through a simple yet effective method of multiplying each expert by the ternary set  $\{-1, 0, 1\}$ , we introduce greater flexibility and diversity into the expert activation process without incurring significant additional costs. Our approach enables more effective use of experts, mitigating issues such as unnecessary activations and underutilization of existing experts that are common in conventional MoE models. Extensive experiments across various benchmarks demonstrate consistent improvements in both effectiveness and efficiency, outperforming existing methods. These results highlight the potential of TC-MoE as a scalable, computationally efficient method for MoE models. We believe this work opens new perspectives for further development in the design and optimization of MoE models, paving the way for more advanced and resource-efficient large-scale models.

540 REFERENCES  
541

- 542 Josh Achiam, Steven Adler, Sandhini Agarwal, Lama Ahmad, Ilge Akkaya, Florencia Leoni Ale-  
543 man, Diogo Almeida, Janko Altenschmidt, Sam Altman, Shyamal Anadkat, et al. GPT-4 technical  
544 report. *arXiv preprint arXiv:2303.08774*, 2023.
- 545 Joshua Ainslie, James Lee-Thorp, Michiel de Jong, Yury Zemlyanskiy, Federico Lebrón, and Sumit  
546 Sanghai. GQA: Training generalized multi-query transformer models from multi-head check-  
547 points. *arXiv preprint arXiv:2305.13245*, 2023a.
- 548 Joshua Ainslie, Tao Lei, Michiel de Jong, Santiago Ontañón, Siddhartha Brahma, Yury Zemlyan-  
549 skiy, David Uthus, Mandy Guo, James Lee-Thorp, Yi Tay, et al. COLT5: Faster long-range  
550 transformers with conditional computation. *arXiv preprint arXiv:2303.09752*, 2023b.
- 551 Yonatan Bisk, Rowan Zellers, Jianfeng Gao, Yejin Choi, et al. PIQA: Reasoning about physical  
552 commonsense in natural language. In *Proceedings of the AAAI Conference on Artificial Intelli-  
553 gence*, 2020.
- 554 Sid Black, Stella Biderman, Eric Hallahan, Quentin Anthony, Leo Gao, Laurence Golding, Ho-  
555 race He, Connor Leahy, Kyle McDonell, Jason Phang, et al. GPT-NeoX-20B: An open-source  
556 autoregressive language model. *arXiv preprint arXiv:2204.06745*, 2022.
- 557 Tom Brown, Benjamin Mann, Nick Ryder, Melanie Subbiah, Jared D Kaplan, Prafulla Dhariwal,  
558 Arvind Neelakantan, Pranav Shyam, Girish Sastry, Amanda Askell, et al. Language models are  
559 few-shot learners. In *Advances in Neural Information Processing Systems*, 2020.
- 560 Christopher Clark, Kenton Lee, Ming-Wei Chang, Tom Kwiatkowski, Michael Collins, and Kristina  
561 Toutanova. BoolQ: Exploring the surprising difficulty of natural yes/no questions. In *Proceedings  
562 of the 2019 Conference of the North American Chapter of the Association for Computational  
563 Linguistics: Human Language Technologies, Volume 1 (Long and Short Papers)*, 2019.
- 564 Peter Clark, Isaac Cowhey, Oren Etzioni, Tushar Khot, Ashish Sabharwal, Carissa Schoenick, and  
565 Oyvind Tafjord. Think you have solved question answering? try arc, the ai2 reasoning challenge.  
566 *arXiv preprint arXiv:1803.05457*, 2018.
- 567 Together Computer. RedPajama: an open dataset for training large language models, 2023. URL  
568 <https://github.com/togethercomputer/RedPajama-Data>.
- 569 Damai Dai, Chengqi Deng, Chenggang Zhao, RX Xu, Huazuo Gao, Deli Chen, Jiashi Li, Wangding  
570 Zeng, Xingkai Yu, Y Wu, et al. DeepSeekMoE: Towards ultimate expert specialization in mixture-  
571 of-experts language models. *arXiv preprint arXiv:2401.06066*, 2024.
- 572 William Fedus, Barret Zoph, and Noam Shazeer. Switch Transformers: Scaling to trillion parameter  
573 models with simple and efficient sparsity. *Journal of Machine Learning Research*, 23(120):1–39,  
574 2022.
- 575 Dan Hendrycks, Collin Burns, Steven Basart, Andy Zou, Mantas Mazeika, Dawn Song, and Jacob  
576 Steinhardt. Measuring massive multitask language understanding. In *International Conference  
577 on Learning Representations*, 2021.
- 578 Quzhe Huang, Zhenwei An, Nan Zhuang, Mingxu Tao, Chen Zhang, Yang Jin, Kun Xu, Kun Xu,  
579 Liwei Chen, Songfang Huang, and Yansong Feng. Harder task needs more experts: Dynamic  
580 routing in MoE models. In *Proceedings of the 62nd Annual Meeting of the Association for Com-  
581 putational Linguistics (Volume 1: Long Papers)*, 2024.
- 582 Robert A Jacobs, Michael I Jordan, Steven J Nowlan, and Geoffrey E Hinton. Adaptive mixtures of  
583 local experts. *Neural Computation*, 3(1):79–87, 1991.
- 584 Albert Q Jiang, Alexandre Sablayrolles, Antoine Roux, Arthur Mensch, Blanche Savary, Chris Bam-  
585 ford, Devendra Singh Chaplot, Diego de las Casas, Emma Bou Hanna, Florian Bressand, et al.  
586 Mixtral of experts. *arXiv preprint arXiv:2401.04088*, 2024.
- 587 Michael I Jordan and Robert A Jacobs. Hierarchical mixtures of experts and the em algorithm.  
588 *Neural Computation*, 6(2):181–214, 1994.

- 594 Dmitry Lepikhin, HyoukJoong Lee, Yuanzhong Xu, Dehao Chen, Orhan Firat, Yanping Huang,  
 595 Maxim Krikun, Noam Shazeer, and Zhifeng Chen. Gshard: Scaling giant models with conditional  
 596 computation and automatic sharding. In *International Conference on Learning Representations*,  
 597 2021.
- 598 Todor Mihaylov, Peter Clark, Tushar Khot, and Ashish Sabharwal. Can a suit of armor conduct elec-  
 599 tricity? a new dataset for open book question answering. In *Proceedings of the 2018 Conference*  
 600 *on Empirical Methods in Natural Language Processing*, 2018.
- 602 Denis Paperno, Germán Kruszewski, Angeliki Lazaridou, Ngoc Quan Pham, Raffaella Bernardi,  
 603 Sandro Pezzelle, Marco Baroni, Gemma Boleda, and Raquel Fernández. The LAMBADA dataset:  
 604 Word prediction requiring a broad discourse context. In *Proceedings of the 54th Annual Meeting*  
 605 *of the Association for Computational Linguistics (Volume 1: Long Papers)*, 2016.
- 606 Guilherme Penedo, Hynek Kydlíček, Loubna Ben allal, Anton Lozhkov, Margaret Mitchell, Colin  
 607 Raffel, Leandro Von Werra, and Thomas Wolf. The FineWeb datasets: Decanting the web for the  
 608 finest text data at scale, 2024. URL <https://arxiv.org/abs/2406.17557>.
- 610 David Raposo, Sam Ritter, Blake Richards, Timothy Lillicrap, Peter Conway Humphreys, and Adam  
 611 Santoro. Mixture-of-Depths: Dynamically allocating compute in transformer-based language  
 612 models. *arXiv preprint arXiv:2404.02258*, 2024.
- 613 Keisuke Sakaguchi, Ronan Le Bras, Chandra Bhagavatula, and Yejin Choi. WinoGrande: An ad-  
 614 versarial winograd schema challenge at scale. *Communications of the ACM*, 64(9):99–106, 2021.
- 616 Maarten Sap, Hannah Rashkin, Derek Chen, Ronan LeBras, and Yejin Choi. SocialIQa: Common-  
 617 sense reasoning about social interactions. In *Proceedings of the 2019 Conference on Empirical*  
 618 *Methods in Natural Language Processing*, 2019.
- 619 Noam Shazeer. Glu variants improve transformer. *arXiv preprint arXiv:2002.05202*, 2020.
- 621 Noam Shazeer, Azalia Mirhoseini, Krzysztof Maziarz, Andy Davis, Quoc Le, Geoffrey Hinton, and  
 622 Jeff Dean. Outrageously large neural networks: The sparsely-gated mixture-of-experts layer. In  
 623 *International Conference on Learning Representations*, 2017.
- 625 Hugo Touvron, Thibaut Lavril, Gautier Izacard, Xavier Martinet, Marie-Anne Lachaux, Timothée  
 626 Lacroix, Baptiste Rozière, Naman Goyal, Eric Hambro, Faisal Azhar, et al. Llama: Open and  
 627 efficient foundation language models. *arXiv preprint arXiv:2302.13971*, 2023.
- 628 An Wang, Xingwu Sun, Ruobing Xie, Shuaipeng Li, Jiaqi Zhu, Zhen Yang, Pinxue Zhao, JN Han,  
 629 Zhanhui Kang, Di Wang, et al. Hmoe: Heterogeneous mixture of experts for language modeling.  
 630 *arXiv preprint arXiv:2408.10681*, 2024.
- 632 Tianwen Wei, Bo Zhu, Liang Zhao, Cheng Cheng, Biye Li, Weiwei Lü, Peng Cheng, Jianhao  
 633 Zhang, Xiaoyu Zhang, Liang Zeng, et al. Skywork-MoE: A deep dive into training techniques for  
 634 mixture-of-experts language models. *arXiv preprint arXiv:2406.06563*, 2024.
- 635 Shaohua Wu, Jiangang Luo, Xi Chen, Lingjun Li, Xudong Zhao, Tong Yu, Chao Wang, Yue Wang,  
 636 Fei Wang, Weixu Qiao, et al. Yuan 2.0-M32: Mixture of experts with attention router. *arXiv*  
 637 *preprint arXiv:2405.17976*, 2024.
- 639 Guangxuan Xiao, Yuandong Tian, Beidi Chen, Song Han, and Mike Lewis. Efficient streaming  
 640 language models with attention sinks. In *International Conference on Learning Representations*,  
 641 2024.
- 642 Yuanhang Yang, Shiyi Qi, Wencho Gu, Chaozheng Wang, Cuiyun Gao, and Zenglin Xu. XMoE:  
 643 Sparse models with fine-grained and adaptive expert selection. In *Findings of the Association for*  
 644 *Computational Linguistics: ACL 2024*, 2024.
- 646 Rowan Zellers, Ari Holtzman, Yonatan Bisk, Ali Farhadi, and Yejin Choi. Hellaswag: Can a ma-  
 647 chine really finish your sentence? In *Proceedings of the 57th Annual Meeting of the Association*  
 648 *for Computational Linguistics*, 2019.

648 Zihao Zeng, Yibo Miao, Hongcheng Gao, Hao Zhang, and Zhijie Deng. AdaMoE: Token-  
 649 adaptive routing with null experts for mixture-of-experts language models. *arXiv preprint*  
 650 *arXiv:2406.13233*, 2024.

651  
 652 Biao Zhang and Rico Sennrich. Root mean square layer normalization. In *Advances in Neural*  
 653 *Information Processing Systems*, 2019.

654  
 655 Yanqi Zhou, Tao Lei, Hanxiao Liu, Nan Du, Yanping Huang, Vincent Zhao, Andrew M Dai, Quoc V  
 656 Le, James Laudon, et al. Mixture-of-experts with expert choice routing. In *Advances in Neural*  
 657 *Information Processing Systems*, 2022.

658  
 659 Barret Zoph, Irwan Bello, Sameer Kumar, Nan Du, Yanping Huang, Jeff Dean, Noam Shazeer, and  
 660 William Fedus. ST-MoE: Designing stable and transferable sparse expert models. *arXiv preprint*  
 661 *arXiv:2202.08906*, 2022.

## 662 A APPENDIX

### 663 A.1 CALCULATING THE CONTRIBUTION OF EACH ACTIVATION

664 To evaluate the effectiveness of the routing scheme, we conduct experiments to analyze the impact of  
 665 routing decisions on model outputs. It is important to note that we are not discussing the contribution  
 666 of each expert, but rather the effect of each individual activation decision made by the router.

667 Specifically, we first randomly select 15 sequences from the training set of RedPajama (Computer,  
 668 2023) and the test set of ARC-Easy (Clark et al., 2018), respectively. The average sequence length  
 669 of samples in the training set is 1608, while it is 30 in the test set. We use the language modeling  
 670 loss on these sequences to measure the quality of model outputs. For a specific activation  $A$ , a  
 671 straightforward method to obtain its contribution is to forward the model on the input sequence  
 672 twice: once with this activation and once masking this activation. We then calculate the difference  
 673 in the loss function. This can be formulated as follows:

$$674 \text{Contribution}_A := \mathcal{L}(M_{\setminus\{A\}}(x)) - \mathcal{L}(M(x)), \quad (14)$$

675 where  $x$  denotes the input sequence,  $\mathcal{L}$  denotes the loss function,  $M$  denotes the function of the  
 676 model, and  $M_{\setminus\{A\}}$  denotes the function of the model when masking the activation  $A$ . For sequences  
 677 sampled from the pre-trained data, we compute the loss across all positions, whereas for sequences  
 678 sampled from the test data, we calculate the loss only over the tokens constructing the answer. When  
 679 masking activation  $A$  results in a higher loss, we calculate a positive contribution for activation  $A$ .  
 680 This indicates that the activation decision has a beneficial impact on model performance.

681 However, we observe empirically that the impact of masking a single activation is too small to  
 682 analyze effectively. Therefore, we alternatively categorize the activations into groups based on their  
 683 gate values and calculate the contribution of each group. Specifically, we divide the gate values  
 684 from 0 to 1 into 10 intervals: 0 to 0.1, 0.1 to 0.2, ..., 0.9 to 1.0. Nevertheless, the unequal size of  
 685 different groups still makes it unfair to compare the contributions across groups. To address this, we  
 686 randomly select the same number of activations to mask within each group for a fair comparison.  
 687 Specifically, we mask 20 activations in each layer of each group for sequences sampled from the  
 688 training set, and 5 activations in each layer of each group for sequences sampled from the test set.  
 689 We then calculate the loss difference as shown in Equation 14.

690 For the experiments involving the flipping of expert output signs, we use a similar method. For a  
 691 specific activation  $A$ , we forward the model on the input sequence twice: once with this activation  
 692 and once with the flipped sign activation, then calculate the difference in the loss function. We define  
 693 this as:

$$694 \text{Contribution}_{-A} := \mathcal{L}(M_{\setminus\{A\}, \cup\{-A\}}(x)) - \mathcal{L}(M(x)), \quad (15)$$

695 where  $M_{\setminus\{A\}, \cup\{-A\}}$  denotes the function of the model when the sign of activation  $A$  is flipped. We  
 696 randomly flip the sign of 20 activations with gate values lower than 0.2 in each layer, obtaining the  
 697 distribution shown in Figure 1b.

702    A.2 HYPER-PARAMETERS  
 703

704    We use the AdamW optimizer with a first-moment decay of  $\beta_1 = 0.9$  and a second-moment decay  
 705    of  $\beta_2 = 0.95$ . The weight decay is set to 0.1 in our experiments. The learning rate is gradually  
 706    increased from 0 to 3e-4 in the first 10% of training steps and then decays to 3e-5 using a cosine  
 707    decay schedule for the remaining steps. We set the sequence length to 2048 and the global batch  
 708    size to 2048.

709    To achieve a flexible trade-off between effectiveness and efficiency for Random Drop, Top-P, and  
 710    TC-MoE, we tune specific hyperparameters:  
 711

- 712    • **Random drop:** We set the drop probability  $p$  to 15%, 45%, and 70% to achieve average  
 713    activation numbers of 1.85, 1.55, and 1.30, respectively.
- 714    • **Top-P:** We set the threshold  $P$  to 0.4 as in the original paper (Huang et al., 2024), and the  
 715    dynamic loss weight to 1e-5, 2e-5, and 5e-5 to achieve average activation numbers of 1.99,  
 716    1.56, and 1.14, respectively.
- 717    • **TC-MoE:** We set the load balance factor  $\alpha_1$  to 0.01, and the reward factor  $\alpha_2$  to 0, 1e-5,  
 718    and 2e-5 to achieve average activation numbers of 1.82, 1.61, and 1.30, respectively.

721    For initialization, we adopt an initializer range of 0.006. The weight matrix  $W_g$  of the router is also  
 722    initialized with a standard deviation of 0.006. The bias term  $b_g \in \mathbb{R}^{2N+K}$  of the router is initialized  
 723    with 0 for experts of type  $E^1$ , -1 for experts of type  $E^{-1}$ , and -10 for experts of type  $E^0$ . This  
 724    initialization is designed to make the router concentrate on type  $E^1$  at the beginning of the training  
 725    process.

726    A.3 IMPROVING THE TOP-K ROUTING SCHEME  
 727

729    Intuitively, experts from  $E^0$  share similarities with attention sinks (Xiao et al., 2024). The intuition  
 730    behind attention sinks is that the attention scores calculated by the Softmax operation sum up to  
 731    one for all tokens. As a result, the model naturally learns to assign useless attention scores to sink  
 732    tokens. Similarly, in MoE models, the Softmax operation is used by the router to calculate gate  
 733    values. Therefore, we believe that experts from  $E^0$  serve as sink experts in this case to collect  
 734    unneeded gate values.

735    However, in the classical Top-K routing mechanism, as demonstrated in Equation 10, only the activated  
 736    experts participate in the competition for the gate values. This means that experts from  $E^0$  are  
 737    effective only when they are among the Top-K experts. To address this, we improve our design by  
 738    always activating experts of type  $E^0$ , allowing them to participate fully in the competition for gate  
 739    values and better serve as sinks. Specifically, we modify the activation set  $\mathcal{E}$  by taking the union  
 740    with  $E^0$ . The updated calculation of gate values is formulated as follows:

$$741 \quad g_i(\mathbf{h}) = \begin{cases} p_i(\mathbf{h}) / \sum_{j \in \mathcal{E} \cup E^0} p_j(\mathbf{h}), & i \in \mathcal{E} \cup E^0 \\ 0, & i \notin \mathcal{E} \cup E^0 \end{cases} \quad (16)$$

745    where  $\mathcal{E}$  denotes the set of the top  $K$  experts with the highest probabilities.  
 746

748    A.4 EFFECT OF THE REWARD LOSS  
 749

750    We also investigate the effect of our designed reward loss. As illustrated in Figure 9, we vary the  
 751    reward factor from 0 to 2e-5. The average number of activated experts shows different changing  
 752    curves. By increasing the reward factor, we encourage the model to select experts from  $E^0$ , which  
 753    incur no computational cost. Consequently, the model tends to have a lower average number of  
 754    activated experts. Specifically, the average number of activated experts converges to 1.82 when the  
 755    reward factor is 0 and to 1.30 when the reward factor is 2e-5. These results demonstrate that tuning  
 the reward factor enables a flexible trade-off between effectiveness and efficiency.

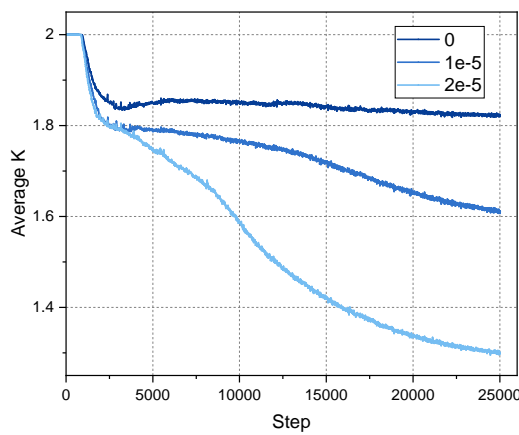


Figure 9: The changing curves of the average number of activated experts when varying the reward factor.

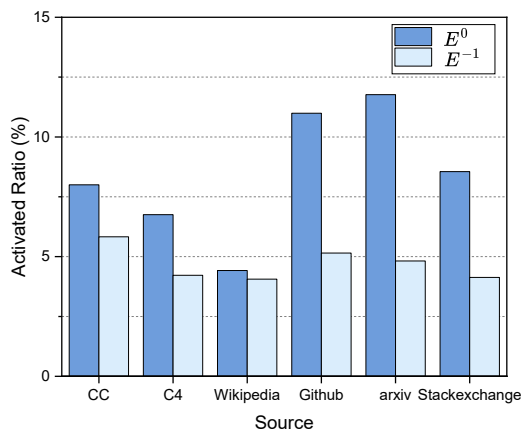


Figure 10: The activated ratios across different sources of training data.

#### A.5 ACTIVATED RATIO ON DIFFERENT SOURCES

We also investigate the activated ratio on different sources of training data. The results are shown in Figure 10. We observe that the activated ratio of  $E^0$  exhibits significant variance across different sources. Notably, The activated ratio of  $E^0$  is around 11% on data from Github and arxiv, while it is only 4% on data from Wikipedia. Similarly, the activated ratio of  $E^{-1}$  also varies across different sources. The activated ratio of  $E^{-1}$  is only 4% on data from Wikipedia and Stackexchange, while it is 6% on data from CC. The variance across different sources indicates some specialization of experts from  $E^0$  and  $E^{-1}$ .